



## AN INVESTIGATION OF PARAMETRIC ARRAY LOUD-SPEAKERS FOR ACTIVE NOISE CONTROL IN A L-SHAPED DUCT

Shuaibing Wu, Ming Wu, Jun Yang

*Key Laboratory of Noise and Vibration Research and Communication Acoustic Laboratory,  
Institute of Acoustics, Chinese Academy of Sciences, Beijing, China 100190*

*e-mail: junyang.ioa@gmail.com*

In order to solve the problem that the acoustic feedback cause the raise of the complexity of the system and computation of algorithms in active noise control of ducts, the parametric array loudspeakers are introduced as the secondary source in this paper. The high directivity sound beam helps parametric array loudspeakers reduce the acoustic feedback. In order to verify the method, active noise control experiments of parametric array loudspeakers using as a secondary source in L-shaped ducts have been completed for single frequency noise and bifrequency noise. Furthermore, regions and areas of noise attenuation have been measured. The experimental results show that the acoustic feedback becomes smaller for parametric array loudspeakers using as the secondary source. Without using feedback compensation, the noise reduction of parametric array loudspeakers is equal with coil loudspeakers' for the single frequency noise; whereas it is relatively imperfect for the bifrequency noise. The noise reduction regions are the entire downstream duct from error microphone, and the noise reduction areas cover the cross-section of the duct. The experiments demonstrate that the noise reduction effectiveness is well and the complexity of the system and computation of algorithms are reduced, under the condition of the parametric array loudspeakers used as secondary source.

---

### 1. Introduction

Active Noise Control (ANC) is greatly superior in size and cost, compared with Passive Noise Control. For the reason, it has been widely applied in the field of noise reduction. In feedforward ANC of the duct, the sound emitted by the secondary source not only cancels noise in the downstream duct, but also radiates upstream to the reference microphone, then confuses the reference signal. This is known as acoustic feedback and the path between secondary source and the reference microphone is defined as acoustic feedback path. The acoustic feedback will reduce the performance of noise control, and result in systems diverging even more. Therefore, it is significant to solve the acoustic feedback. Generic methods to suppress the acoustic feedback include the acoustic feedback neural networks, the location optimization of reference microphone, and the directivity of secondary source.

The acoustic feedback neural network is similar to the echo cancellation<sup>1</sup> in telephone systems in which the acoustic feedback physics path is subtracted by acoustic feedback path modelling which can be achieved either offline<sup>2</sup> or online<sup>3</sup>. Using offline modelling, the neural network con-

sumes fewer resources, but it is susceptible by the fluctuation of acoustic feedback physics path. The online modelling makes the neural network adjust as the acoustic feedback physics path changes; however it inevitably complicates the system and affects the system stability.

In terms of location optimization of reference microphone, Hamada *et al.*<sup>4</sup> proposed that reference microphone and error microphone were placed symmetrically on the secondary source. Then the feedback signal was removed by the subtraction of two microphone signals. Kuo<sup>5</sup> gave alternate way to reduce the acoustic feedback, which he placed the secondary source in the branch duct 45° angle with the main duct. In summary, the performances of these methods were unfavourable.

It is another method to cancel acoustic feedback by use of the characteristics of the sound source directivity. Jessel<sup>6</sup> and Sha *et al.*<sup>7</sup> designed a dipole in orthogonal direction as secondary source for ANC in ducts. The directivity of dipole helped to decrease acoustic feedback. However, the dipole loudspeakers require respective hardware parts, which brought the bulkiness and the complexity of the system. In addition, Swinbanks<sup>8</sup> used multi-pole system for ANC, which included two or more ring-shaped sound source, each of which was composed of four loudspeakers. The aim was to get a better directivity, but the volume of the system became bulky.

Parametric array loudspeakers (PAL) enable high directivity sound along the radiation direction to be generated by the nonlinear effects of ultrasonic waves in air<sup>9</sup>. According to this feature, the research of PAL as a secondary source of ANC has been concerned broadly. Brooks *et al.*<sup>10</sup> investigated the feasibility of PAL applied to ANC through combination of theoretical analysis and experiment. Kider *et al.*<sup>11</sup> studied PAL and virtual sensors applied to localized active sound control in theory. Tanaka *et al.*<sup>12, 13</sup> conducted single-frequency ANC using a steerable PAL and obtained better results.

Certain progresses have been made about PAL used for ANC in free field. However the PAL used for ANC in ducts need to be studied. In this paper, the PAL used as secondary source for ANC in ducts will be studied, in order to decrease the acoustic feedback and reduce the algorithms complexity.

This paper is divided into four sections. Section 2 presents the description of ANC system; Section 3 details the measurement of noise reduction, in terms of hardware platform, experiment configuration, and experiment results. Finally, the conclusion is shown in section 4.

## 2. ANC system

A block diagram of single-channel feedforward ANC systems with a neural network is shown in Figure 1. Here  $P(z)$  is the primary path between the noise source and the error microphone,  $S(z)$  and  $\hat{S}(z)$  are the secondary path and the corresponding modelling between secondary source and the error microphone.  $F(z)$  and  $\hat{F}(z)$  are the feedback path and the corresponding modelling from the secondary source to the reference microphone. The filtered-x LMS (FxLMS) algorithm<sup>14</sup> is used to adapt the ANC adaptive filter  $W(z)$ . The ANC system uses the reference microphone to pick up the reference noise  $r(n)$ , processes this input with an adaptive filter to generate an antinoise  $y(n)$  to cancel the primary noise acoustically in a duct, and uses an error microphone to measure the error  $e(n)$  and to update the adaptive filter coefficients.  $x(n)$  is the acoustic feedback signal.

In the case of dashed box not present in Figure 1, the error signal z-transform is expressed as

$$E(z) = P(z)X(z) + S(z) \frac{W(z)X(z)}{1 - W(z)F(z)}. \quad (1)$$

Assuming that the system converges, the  $W(z)$  must satisfy the following equation

$$W^{\circ}(z) = -\frac{P(z)}{S(z) - P(z)F(z)}. \quad (2)$$

It can be also obtained that the open loop transfer function is

$$H_{OL}(z) = W(z)F(z). \quad (3)$$

Due to the acoustic feedback, The ANC system will be unstable if the coefficients of  $W(z)$  are large enough so that  $W(z)F(z) = 1$  at some frequency.

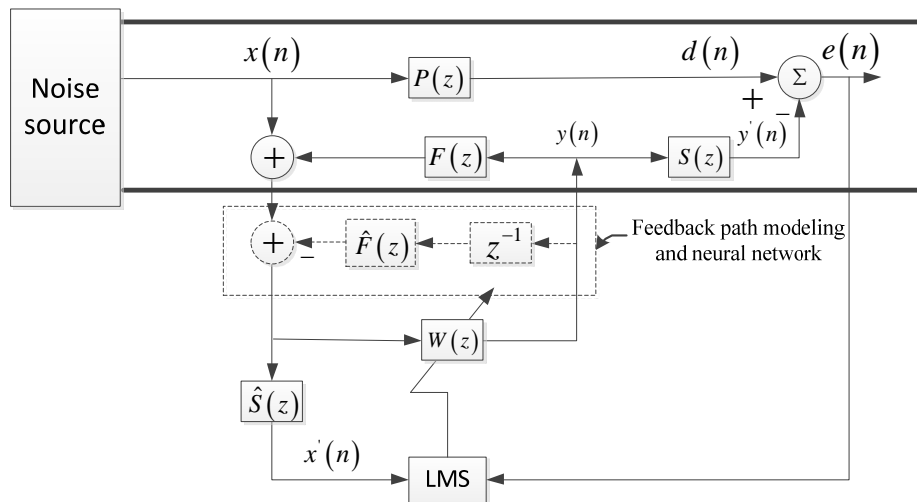


**Figure 1.** Block diagram of single-channel feedforward ANC system.

In order to ensure the system stability, the problem of acoustic feedback must be solved. An approach is to add the neural network while loudspeakers are used as the secondary source; in this paper, another one is proposed that the PAL will be used as a secondary source without using the neural network. The effect of method proposed by us will be validated by the experimental studies.

Real-time experiments are carried out in order to make a comparison of the amount of noise reduction achieved by the three cases, as seen in Tab. 1. The second column of Tab. 1 indicates that the secondary source is either coil loudspeaker (CL) or PAL; the third column point out the algorithms used in the three different cases. The neural network is the component of dotted box in Fig. 1.

**Table 1.** Cases of real-time experiments

Case	Secondary source	Algorithm
I	CL	FxLMS without neural network
II	CL	FxLMS with neural network
III	PAL	FxLMS without neural network

### 3. Measurements of noise reduction

#### 3.1 Hardware platform

The FxLMS algorithm was implemented on a TMS320C6713 signal processor for active noise control. The TMS320C6713 is a high performance, floating-point DSP chip that reaches 2400MIPS and supports 300 MHz clock rates. The analog-to-digital conversion and digital-to-analog conversion are implemented by the ADS8365 and DAC8544 respectively. ADS8365 and

DAC8544 support about 10MHz sampling rate and 16 bits conversion accuracy. Taking into account the frequency of the noise and the computation of the processor, the sampling frequency is designed as 16 kHz. The coefficient values of  $W(z)$  are automatically adjusted according to changes of the acoustic noise sources and environmental parameters, the coefficient numbers is configured as 20 besides. The update step size of coefficient is small enough so as to display the performance comparison of both methods.

### 3.2 Measurements configuration

Noise, generated by the ventilating fan is transmitted through the duct into the working and living environment. Typically, a large number of right-angle corners appear in ventilation systems. The experiment duct in this paper is designed based on the right-angle corner structure, which is shown in Fig. 2. This type duct is named as L-shaped duct in this paper. It is made from 1 cm hard plastic, and the cross-section is a 10 cm X 10 cm rectangular. The SPL of primary noise is about 70 dB. The sizes of CL and PAL are  $\phi 3.5$  cm and 6 cm X 6 cm, respectively. Here, the secondary source is located at the corner and the noise source is situated at the upstream duct from the corner of 100 cm. The reference microphone and error microphone are at 55 cm and 155 cm away from a secondary source, respectively. At the end of the L-shaped duct, the damping material is placed to prevent influence from reflecting. Furthermore, an acoustic filter<sup>15</sup> is used to remove spurious sound generated at the surface of microphones.

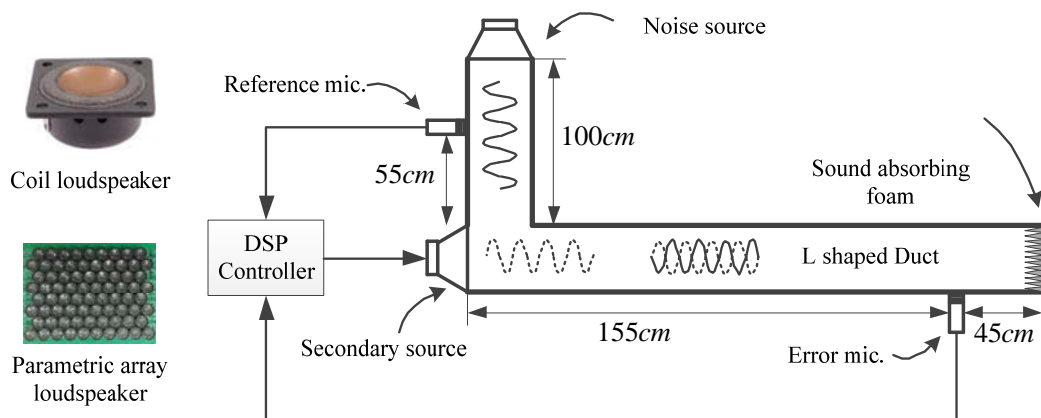
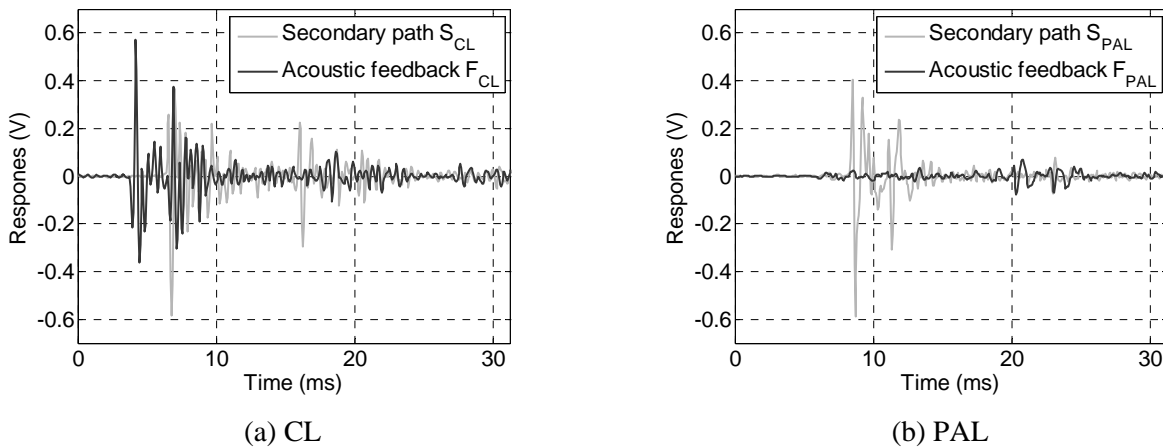


Figure 2. Experimental setup.

### 3.3 Measurements results

Base on the experimental setup, the impulse responses of a secondary path and an acoustic feedback are identified using impulse response measurement for the CL and the PAL, as shown in Fig. 3. The impulse response of the secondary path  $S_{CL}$ , obtained with the classical CL secondary source is compared with the impulse response of the feedback path  $F_{CL}$ , obtained with the classical CL secondary source in Fig. 3(a). The impulse response of the feedback path with CL configuration has a pronounced negative peak about 0.58 V at 7 ms. The amplitude of the feedback impulse is almost equal to the amplitude of the secondary path impulse. Acoustic feedback is significant. The impulse response of the secondary path  $S_{PAL}$ , obtained with the classical PAL secondary source is compared with the impulse response of the feedback path  $F_{PAL}$ , obtained with the classical PAL secondary source in Fig. 3(b). The impulse response of feedback path with PAL configuration has a negative peak about 0.08 V at 20 ms. Compared with  $S_{CL}$ , the ratio between secondary path and acoustic feedback for  $S_{PAL}$  is improved about 17.5 dB. Obviously, the acoustic feedback is decreased enormously using PAL as secondary source.



**Figure 3.** Impulse responses of a secondary path and an acoustic feedback.

The results of ANC experiments are presented in Fig. 4 and Fig. 5. In Fig. 4, a performance of ANC systems of three cases for single frequency (800 Hz) noise is presented. In Fig. 5, a performance of ANC systems of case II and case III for bifrequency (600 Hz and 1200 Hz) noise is presented. The ANC system of case I diverges for bifrequency noise, thus its results is not presented in Fig. 5.

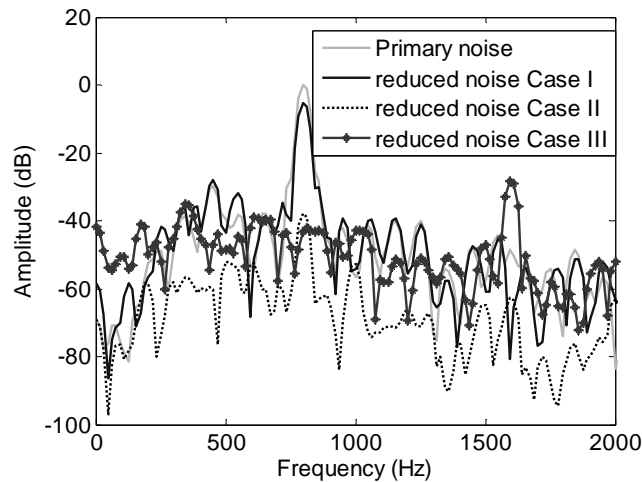


**Figure 4.** Frequency spectra of single frequency noise and residual noise at error microphone position of three cases.

Compared with results of three cases in Fig. 4, it can be clearly seen that the noise reduction amounts of case I, case II and case III are about 5 dB, 38 dB and 42 dB. Obviously, the performance of case I is the worst. The noise reduction amount of case II is slightly less than case III, but due to the linearity of CL better than PAL, the residual noise energy of case II is lower than case III, especially at the frequency of 1600 Hz. The frequency of 1600 Hz is the secondary harmonic of 800 Hz. Nonlinear distortion of PAL impacts more to noise reduction effect of the complicated noise. In the term of algorithm complexity, case I and case III consume the same resource, but less than case II. Therefore, the PAL achieves best noise reduction effect for single frequency at the minimum amount of computation resource.

It can be clearly seen from Fig. 5 that the ANC experiment of case I cannot achieve the noise reduction due to the system diverging; the noise reduction amounts of case II are 41 dB and 44 dB at the frequencies of 600 Hz and 1200 Hz respectively; the noise reduction amounts of case III are 30 dB and 33 dB at the frequencies of 600 Hz and 1200 Hz respectively. Due to harmonic distortion and intermodulation distortion, the performance of case III is less than case II. However, in the term of algorithm complexity, case III still consume less resource than case II. Though the results are affected by nonlinear distortion, the noise reduction performance of the PAL is relatively well, and the amount of consumed computation resource is least.

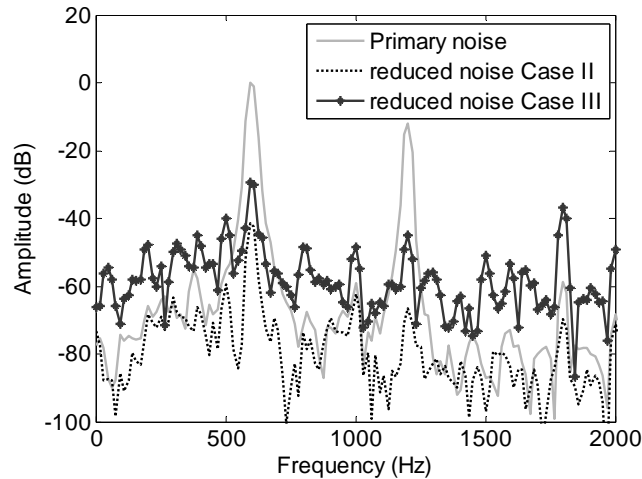


**Figure 5.** Frequency spectra of bifrequency noise and residual noise at error microphone position of case II and case III.

As the theory is different between PAL and CL, the noise reduction regions and areas in case III require to be validated. The experimental setups for validation are shown in Fig.6.

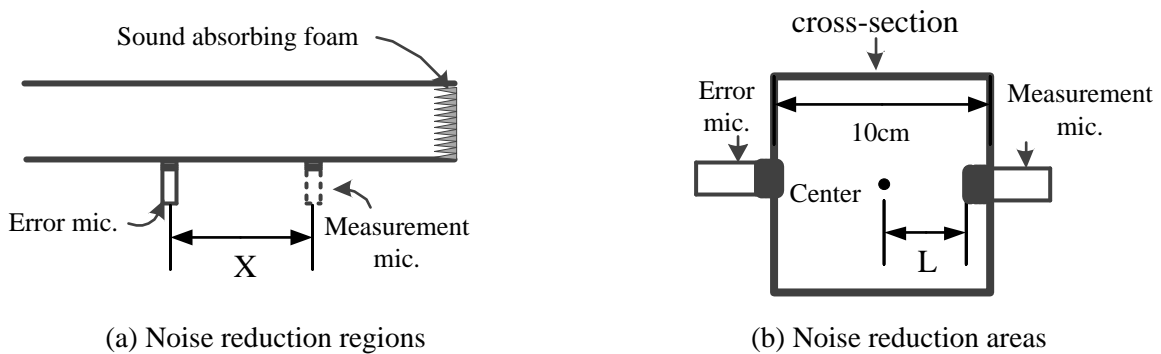


**Figure 6.** The experimental setups for validation of noise reduction regions and areas.

Firstly, the reduction regions are measured for 800 Hz noise, as shown in Fig. 6(a). The measurement microphone is distributed at the position of  $X = 10\text{ cm}$ ,  $20\text{ cm}$ ,  $30\text{ cm}$  and  $40\text{ cm}$ , respectively. The results are listed in Tab. 2. It is seen that the amounts of noise reduction at  $X = 10\text{ cm}$ ,  $20\text{ cm}$ ,  $30\text{ cm}$  and  $40\text{ cm}$  are relatively stable, but slightly less than that measured by error microphone. The reason is that the linear modelling of secondary path for PAL produces errors in other locations.

Next, the reduction areas are measured for 800 Hz noise, as shown in Fig. 6(b). The measurement microphone and error microphone are installed in the same cross-section. As the duct is symmetrical, it is only needed to measure the results between center point and one wall.  $L = 0\text{ cm}$

means that the measurement microphone is located at the center point,  $L = 5$  cm means that the microphone is flush with inside wall. The results are listed in Tab. 3. It is seen that the amounts of noise reduction at  $L = 0 \sim 5$  cm are almost equal and present small fluctuation. It can be concluded by experiments that the noise reduction regions can cover the downstream duct from error microphone and the noise reduction areas can cover the whole cross-section, using PAL as secondary source.

**Table 2.** Noise reduction regions

X (cm)	10	20	30	40
Amount of noise reduction (dB)	28	26	29	32

**Table 3.** Noise reduction areas

L (cm)	0	1	2	3	4	5
Amount of noise reduction (dB)	42	40	39.5	40.5	39.5	40

## 4. Conclusions

In this article, it was demonstrated that a PAL enables the secondary source high directivity and reduces the acoustic feedback. At the same time, the PAL can be employed as a secondary source for ANC systems and makes significant noise reduction amounts for single frequency and bifrequency noise without using neural network. It is important that the PAL used as the secondary source decreases the amount of computation resource. Finally, the reduction regions and areas of the PAL can cover the entire duct downstream from error microphone by the validation experiment.

As the nonlinear distortion exists, the PAL cannot be used for broadband noise control. In the future work, we will majorly study algorithms to reduce the nonlinear distortion and nonlinear noise control algorithms for PAL.

## 5. Acknowledgments

We would like to thank Fengyan An, Yin Cao and Zheng Kuang for their very useful suggestions. This work was partially supported by NNSF of China under Grants (11004217, 11074279 and 11174317).

## REFERENCES

- <sup>1</sup> M.M. Sondhi, D.A. Berkley, Silencing echoes on the telephone network, *Proceedings of the IEEE*, **68** (8), 948-963 (1980).
- <sup>2</sup> L. Poole, G. Warnaka, R. Cutter, The implementation of digital filters using a modified Widrow-Hoff algorithm for the adaptive cancellation of acoustic noise, *Acoustics, Speech, and Signal Processing, IEEE International Conference on ICASSP'84.*, San Diego, California, 19-21 March, (1984).
- <sup>3</sup> M.T. Akhtar, M. Abe, M. Kawamata, W. Mitsuhashi, A simplified method for online acoustic feedback path modeling and neutralization in multichannel active noise control systems, *Signal Processing*, **89** (6), 1090-1099 (2009).
- <sup>4</sup> H. Hamada, T. Miura, M. Takahashi, Y. Oguri, An adaptive noise control system in air - conditioning ducts, *The Journal of the Acoustical Society of America*, **84** (S1), S180-S180 (1988).

- <sup>5</sup> S.M. Kuo, J. Tsai, Arrangements of the secondary source on the performance of active noise control systems, *Circuits and Systems, 1993., ISCAS'93, 1993 IEEE International Symposium on*, 3-6 May, (1993).
- <sup>6</sup> M. Jessel, G. Mangiante, Active sound absorbers in an air duct, *Journal of sound and vibration*, **23** (3), 383-390 (1972).
- <sup>7</sup> S. Jia-zhen, S. Guang-rong, C. Shui-xuan, W. Qi-xue, Active sound absorber in ducts, *ACTA ACUSTICA*, **3** (5), 137-141 (1981).
- <sup>8</sup> M.A. Swinbanks, The active control of sound propagation in long ducts, *Journal of Sound and Vibration*, **27** (3), 411-436 (1973).
- <sup>9</sup> J. Yang, W.-S. Gan, K.-S. Tan, M.-H. Er, Acoustic beamforming of a parametric speaker comprising ultrasonic transducers, *Sensors and Actuators A: Physical*, **125** (1), 91-99 (2005).
- <sup>10</sup> L.A. Brooks, A.C. Zander, C.H. Hansen, Investigation into the feasibility of using a parametric array control source in an active noise control system, *Proceedings of ACOUSTICS*, Busselton, Western Australia, 9-11 November, (2005).
- <sup>11</sup> M.R.F. Kidner, C. Petersen, A.C. Zander, C.H. Hansen, Feasibility study of localised active noise control using an audio spotlight and virtual sensors, *Proceedings of ACOUSTICS*, Christchurch, New Zealand, 20-22 November, (2006).
- <sup>12</sup> N. Tanaka, M. Tanaka, Active noise control using a steerable parametric array loudspeaker, *The Journal of the Acoustical Society of America*, **127** (6), 3526-3537 (2010).
- <sup>13</sup> N. Tanaka, M. Tanaka, Mathematically trivial control of sound using a parametric beam focusing source, *The Journal of the Acoustical Society of America*, **129** (1), 165-172 (2011).
- <sup>14</sup> S.M. Kuo, D.R. Morgan, Active noise control: a tutorial review, *Proceedings of the IEEE*, **87** (6), 943-973 (1999).
- <sup>15</sup> C. Ye, Z. Kuang, M. Wu, J. Yang, Development of an Acoustic Filter for Parametric Loudspeaker in Air, *Japanese Journal of Applied Physics*, **50** (7), 07HE18-07HE18-02 (2011).